

Urate Oxidase (UOx)-Copper Oxide (CuO)-Carbon Polymer Composite Electrode for Electrochemical Detection of Uric Acid

Angelo Gabriel E. Buenaventura

Allan Christopher C. Yago*

Institute of Chemistry

University of the Philippines Diliman

Natural Sciences Research Institute

University of the Philippines Diliman

ABSTRACT

This study presents an electrochemical biosensor developed for uric acid (UA) determination using carbon paste electrode (CPE) modified with copper (II) oxide (CuO) particles and urate oxidase (UOx) enzyme. Base CPE is prepared using a multi-walled carbon nanotube (MWCNT) and a polydimethylsiloxane (PDMS) binder. The main sensing process is based on the oxidation of UA into 5-hydroxyisourate (HIU) as catalyzed by UOx, forming H_2O_2 as byproduct, and then the H_2O_2 reduction-oxidation (redox) reaction converts CuO to form Cu_2O ; the amount of H_2O_2 and hence UA in the sample is measured by the oxidative current measured for the conversion of Cu_2O back to CuO. Cyclic Voltammetry (CV) measurements revealed that the activity of UOx was retained with an apparent Michaelis constant (K_m^{app}) to be equal to 41.46 μM . Differential Pulse Voltammetry (DPV) measurements of UA using UOx-CuO-CPE showed a linear response ranging from 10 μM to 79.4 μM UA with a limit of detection (LOD) determined to be equal to 8.82 μM . UOx-CuO-CPE was shown to be selective towards UA even in the presence of creatinine, xanthine, and glucose. Furthermore, UOx-CuO-CPE was shown to be reusable (3.28% RSD), and its fabrication is repeatable using single factor Analysis of Variance (ANOVA) [$F(1.396) < F_{critical}(5.143)$]. UOx-CuO-CPE was also shown to be stable even after five weeks of storage using the two-sample t-test [$t(0.156) < t_{critical}(4.303)$]. Based on a recovery test using synthetic urine sample, this study showed the applicability of UOx-CuO-CPE in the detection of UA in human urine with 90.27%–102.03% recovery ($n = 3$).

Keywords: Urate Oxidase, Copper (II) Oxide, Carbon Paste Electrode, Uric Acid

* Corresponding Author

INTRODUCTION

Uric acid (UA) is the end-product of purine catabolism of higher primates including humans (Walker et al. 1990). Normal UA levels in blood for premenopausal females range from 2.6-6.0 milligram per deciliter (mg/dL) and 3.5-7.2 mg/dL for males and postmenopausal females (Desideri et al. 2014). Excess UA is normally excreted in urine. In normal adults consuming an average diet, the normal UA secretion in urine is 800 mg or less over 24 hours (Suki and Massry 2012). Abnormal levels of UA have been associated with several diseases such as gout (Perez-Ruiz et al. 2015), hypertension (Feig and Johnson 2003; Masuo et al. 2003), metabolic syndrome (Matsuura et al. 1998; Ishizaka et al. 2005), diabetes (Nakanishi et al. 2003), kidney disease (Obermayr et al. 2008), cardiovascular disease (Bickel et al. 2002), Hodgkin's disease (Kay and Gottlieb 1973), Fanconi syndrome (Ben-Ishay et al. 1961), and medullary thyroid cancer (Puig et al. 1984). Due to these associations of UA level with various diseases, UA analysis has become a routine test in clinical laboratories. Two clinical methods are currently accepted for UA determination (Walker et al. 1990; Watts 1974). One is the colorimetric method which involves the reduction of chromagen such as sodium tungstate with UA to produce a measurable color change. This method is generally considered to give an overestimate of the true value of UA. Another method is the UV differential absorption of UA using uricase or urate oxidase (UOx), and then UOx catalyzes the conversion of UA to allantoin. This method is more expensive because of the one-way use of UOx. Therefore, there is need to develop a selective and sensitive sensor that can be reused to maximize its cost efficiency. Several sensing methods have been utilized for sensor development for UA determination including electrochemical (Rafati et al. 2014), fluorescence-based (Zhang et al. 2011), colorimetric (Wu et al. 2015), and chemiluminescence (Chaudhari et al. 2012). Among these methods, the electrochemical method is the most widely used for sensor development of UA and other biologically important compounds due to high sensitivity and selectivity, portable field-based size, rapid response time and low cost (Wang et al. 2008). One major problem in the electrochemical detection of UA is the coexistence of electroactive interference in biological fluids such as ascorbic acid (AA), which has similar oxidation potential, $E_{1/2} \approx 200\text{mV}$ versus SCE, at graphite electrodes (Bravo et al. 1998). Biological samples like blood and urine also contain various non-electroactive biochemical compounds that may interfere in UA measurements. Thus, a selective recognition element is required to ensure high selectivity for UA detection. One strategy that can be used is to modify an electrode with an enzyme that has specific interaction with

the analyte. The group of Usman Ali et al. used UOx and ZnO nanorods to fabricate an enzymatic biosensor for UA (Usman Ali et al. 2011). UOx was electrostatically immobilized on gold substrate with chemically grown ZnO nanorods. In another study, an amperometric biosensor for UA was fabricated by immobilizing UOx via glutaraldehyde crosslinking on polyaniline-polypyrrole (PANI-PPY) composite film on the surface of a platinum electrode (Arslan 2008). A similar study was conducted where semiconductor CuO particles and UOx were utilized in the fabrication of an electrochemical biosensor for UA determination (Jindal et al. 2012). In that study, CuO was deposited via Pulse Laser Deposition (PLD) onto a Pt-coated glass substrate. The study reported the biocatalytic property of the immobilized UOx by having low apparent Michaelis constant (K_m^{app}) measured at 0.12 mM. However, the utilized technique of CuO deposition and substrate is complicated and more expensive than the electrodeposition method presented in this paper. Our results showed that a simple UA electrochemical biosensor can be prepared using a UOx-CuO-CPE system with low detection limit (8.82 μ M) and highly selective towards UA. The biosensor showed to have high recovery values (90.27%–102.03%) using synthetic human urine, which indicates its applicability to human urine.

The main goal of the study is to fabricate a selective and sensitive electrochemical biosensor for UA determination using CPE modified with CuO particles and UOx. The specific objectives were as follows: 1) fabricate UOx-CuO-CPE and evaluate its electrochemical response; 2) optimize the sensing parameters for UA determination and evaluate the sensing performance of UOx-CuO-CPE; and 3) perform UA determinations in synthetic urine using UOx-CuO-CPE.

MATERIALS AND METHODS

Chemicals and Instrumentation

Multi-walled carbon nanotube powder (MWCNT) was purchased from Chengdu Organic Chemicals Co. Ltd., Chinese Academy of Sciences (purity: >95%; length 10–30 μ m; internal diameter 5–10 nm and outer diameter 10–20 nm). Copper chloride (CuCl_2) (purity: \geq 98.0%) was purchased from Techno Pharmchem. Boric acid was purchased from UniChem (purity: \geq 99.5%). Sodium hydroxide pellets (NaOH) were purchased from Univar (purity: \geq 97.0%). Sodium phosphate dibasic (Na_2HPO_4) was purchased from Duksan Reagents (purity: \geq 99.0%). Potassium dihydrogen orthophosphate (KH_2PO_4) was purchased from Himedia (purity: \geq 99.5%). Potassium chloride (KCl) was purchased from Alfa Aesar (purity: \geq 99.0%). Sodium chloride

(NaCl) (purity: $\geq 99.0\%$) and potassium ferrocyanide trihydrate $\{K_4[Fe(CN)_6] \cdot 3H_2O\}$ (purity: $\geq 98.5\%$) were purchased from JT Baker. Polydimethylsiloxane liquid (PDMS) with 500 centiStokes (cSt) viscosity, uricase or urate oxidase from *Arthrobacter globiformis* (UOx) (15–30 units/mg), uric acid (UA) (purity: $\geq 99.0\%$), xanthine (purity: $\geq 99.5\%$), creatinine (purity: $\geq 98.0\%$), and D-(+)-Glucose (purity: ACS Reagent) were purchased from Sigma Aldrich. All solutions were prepared using deionized water. Blank and UA sensing solutions were all buffered using borate buffered saline (BBS) composed of 0.1 M borate and 0.2 M NaCl. UOx solutions were prepared by dissolving UOx with BBS at pH 9.0.

All electrochemical measurements, including Cyclic Voltammetry (CV), Chronoamperometry (CA), Electrochemical Impedance Spectroscopy (EIS), and Differential Pulse Voltammetry (DPV), were performed using Autolab PGSTAT 302N with a three-electrode system. The fabricated UOx-CuO-CPE was used as the working electrode; an Ag/AgCl (3.0 M KCl) electrode as the reference electrode; and a platinum (Pt) coated rod as the counter electrode.

Preparation of UOx-CuO-CPE

A CPE composed of MWCNT and 500 cSt PDMS liquid polymer was used as the working electrode. The percentage composition as well as electrochemical pretreatment of the resulting electrode were already optimized in the previous studies of our group (Buenaventura et al. 2016; Buenaventura and Yago 2018). Figure 1 shows the scheme for fabrication of UOx-CuO-CPE. In brief, 0.10 g of MWCNT powder was mixed with 0.90 g of PDMS in an agate mortar and pestle. The resulting composite was packed in a 1-mL plastic tube. A copper wire was inserted in the plastic tube up to about 1 cm from surface, which served as the electrical contact. The surface of the resulting CPE was polished using a glass slide. The CPE then underwent anodization electrochemical pretreatment via CV, which was performed in 0.1 M NaOH solution using the following parameters: scan rate: 100 mV/s, potential window: -0.3 V to +1.5 V, and number of cycles: 30.

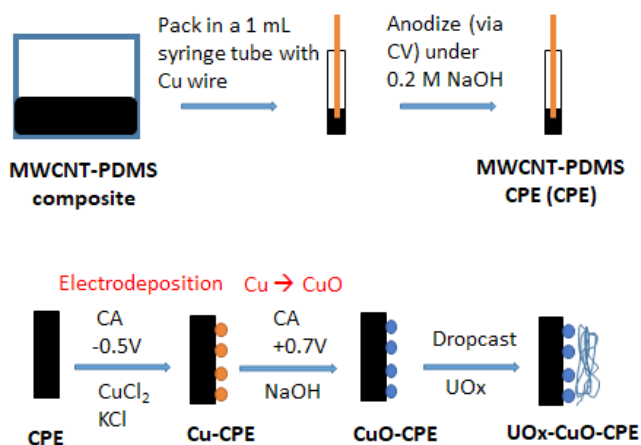


Figure 1. Sensor fabrication scheme for UOx-CuO-CPE.

The fabricated CPE was then further modified in order to fabricate UOx-CuO-CPE. CPE was electrodeposited with CuO to produce CuO-CPE using the same procedure as our previous study on CuO-CPE (Buenaventura and Yago 2020). Copper (Cu) particles were first electrodeposited on the surface of CPE via CA. Using CPE as working electrode in 20 mM CuCl₂ with 0.1M KCl solution, -0.5 V was applied for 20 s. The resulting Cu-CPE was anodized via CA. In 0.1 M NaOH solution, +0.7 V was applied on Cu-CPE for 60 s. The resulting CuO-CPE was then modified with UOx. Onto the surface of CuO-CPE, 45 μ L of 0.3 mg/mL of UOx in BBS (pH 9.0) was dropcasted and was allowed to air-dry for at least 12 hours. The modified electrode was washed with BBS (pH 9.0) then with deionized water to remove loosely bound enzymes. The resulting UOx-CuO-CPE was stored in a refrigerator with a temperature of around 4 $^{\circ}$ C when not in use.

Electrochemical Characterization of CPE, CuO-CPE and UOx-CuO-CPE

Electrochemical measurements were done in order to determine the electrochemical signals towards various solutions using the fabricated biosensor. Electrochemical measurements that were done include Cyclic Voltammetry (CV) and Electrochemical Impedance Spectroscopy (EIS). The parameters for CV measurements that were used are as follows: potential range -0.5 to +0.8 V and 10 mV/s scan rate. The parameters for EIS measurements that were used are as follows: frequency range 0.1 Hz to 20 kHz; applied potential +0.45 V for BBS (pH 8.6) solution and +0.35 V for Fe(CN)₆⁴⁻_(aq) in BBS (pH 8.6) solution.

Optimization of Parameters for Electrochemical Determination of Uric Acid

Different parameters were optimized for UOx-CuO-CPE, including enzyme loading (amount of enzyme dropcasted on the surface of the CuO-CPE), sensing solution pH (pH value of the sensing solution), and equilibration time (amount of time the biosensor was immersed into the sensing solution under stirring condition). For all the optimizations, univariate optimizations were done, i.e. one parameter (which is being optimized) was varied, while the rest of the parameters were held constant. The optimizations were all based on the measured signal towards 79.4 μM UA in BBS (pH 9.0) through CV measurements. The parameter value that gave the highest average peak current (Ave. I_p) was chosen as the optimized value. The optimization of enzyme loading was done via CV measurements using different UOx-CuO-CPEs with different enzyme loading (0.02–0.5 mg/mL UOx in BBS). The optimized value was used for the subsequent optimizations. For the optimization of sensing solution pH, CV measurements of different UA (79.4 μM) sensing solutions with different pH values (pH 8.2–9.4) were done using UOx-CuO-CPEs; one biosensor was used for each pH value. The optimized value was used for the next optimization. For the optimization of equilibration time, UOx-CuO-CPEs were equilibrated in UA sensing solution at different equilibration times (1–5 mins) then CV measurements of UA (79.4 μM) in BBS (pH 8.6) were done afterwards; one biosensor was used for each equilibration time.

Uric Acid Sensing Procedure

UA sensing using UOx-CuO-CPE involves two steps. UOx-CuO-CPE was first dipped into the sensing solution for an optimized period of time under stirring condition. After that, the solution immediately underwent electrochemical measurement for UA sensing. Differential pulse voltammetry (DPV) was used as the electrochemical detection technique for UA sensing using the fabricated UOx-CuO-CPE biosensor. The parameters used for DPV measurements were as follows: initial potential -0.1 V, end potential 0.8 V, scan rate 0.01 V/s, step potential 5 mV, modulation amplitude 25 mV, and modulation time 50 ms. The calibration curve was obtained by measuring the peak height (I_p) from DPV measurements of sensing solutions with varying UA concentrations (10.0–79.4 μM). Three (3) measurements were done for each concentration. After each DPV measurement, an oxidation potential (+0.7 V) via chronoamperometry (CA) in BBS (pH 9.0) was applied in order to re-oxidize remaining Cu_2O to CuO . This was done in order to ensure repeatable measurements.

Selectivity Study

A selectivity study was conducted in order to evaluate the UOx-CuO-CPE response towards UA in the presence of possible interfering species. This was done by measuring UOx-CuO-CPE response towards different solutions with varying compositions as follows: 39.6 μM UA, 39.6 μM UA with 39.6 μM creatinine, 39.6 μM UA with 39.6 μM xanthine, and 39.6 μM UA with 39.6 μM glucose. Measurements were also done using CPE for comparison.

UA Analysis in Synthetic Urine

The UOx-CuO-CPE is intended to be used as a UA sensor in human urine. However, this study is limited to using synthetic urine as representative of human urine. Synthetic urine was prepared with constituents similar to the formulated artificial human urine in a separate study (Khan et al. 2017), and was used for UA analysis. In brief, the prepared synthetic urine has the following components: 9.3g/L urea, 0.670 g/L creatinine, 0.2 g/L KCl, 8 g/L NaCl, 1.14 g/L Na_2HPO_4 , and 0.2 g/L KH_2PO_4 . 1 mL of synthetic urine sample was mixed with 50 mL 0.2 M Borate Buffer (pH 8.6) in 0.4 M NaCl, then diluted with deionized water to produce 100 mL synthetic urine sensing solution. The resulting solution underwent UA measurement using the UOx-CuO-CPE sensor. Separate synthetic urine sensing solutions were spiked with UA at three different spiking levels (7.4 μM , 30 μM , and 55.8 μM). These synthetic urine sensing solutions were prepared by adding an appropriate amount of 10 mM UA in 0.1 M NaOH (stock UA solution) to 1 mL of synthetic urine solution, just before dilution using deionized water. Spiked samples also underwent UA measurement. A recovery study was done in order to assess the matrix effect towards UA sensing using UOx-CuO-CPE. It was done by measuring the percent recovery in the spiked synthetic urine samples using the equation below.

$$\%recovery = \frac{[UA]_{spiked\ sample} - [UA]_{unspiked\ sample}}{[UA]_{added}} \times 100 \quad (1)$$

RESULTS AND DISCUSSION

Fabrication and Optimization Of UOx-CuO-CPE and its UA Sensing Performance

The UOx-CuO-CPE biosensor reported in this study was fabricated using CPE that was previously studied and optimized by our group (Buenaventura and Yago 2018). CuO particles were electrodeposited onto the surface of CPE, producing CuO-CPE. Previous experiments revealed that CuO-CPE can respond towards H_2O_2 via DPV measurements (Buenaventura and Yago 2020). This is because H_2O_2 can reduce CuO to Cu_2O spontaneously. The Cu_2O can be oxidized back to CuO upon application of suitable oxidation potential. For the CuO-CPE to selectively respond with UA, the surface of CuO-CPE was further modified with UOx. The resulting electrode will be termed here as UOx-CuO-CPE. As shown in figure 2A, UOx can catalyze the oxidation of UA, where H_2O_2 is a byproduct. Figure 2B shows the sensing mechanism of UOx-CuO-CPE for UA detection. The main sensing process is based on the oxidation of UA into 5-hydroxyisourate (HIU) as catalyzed by UOx, forming H_2O_2 as byproduct, and then the H_2O_2 redox reaction converts CuO to form Cu_2O ; the amount of H_2O_2 and hence UA in the sample is measured by the oxidative current measured for the conversion of Cu_2O back to CuO.

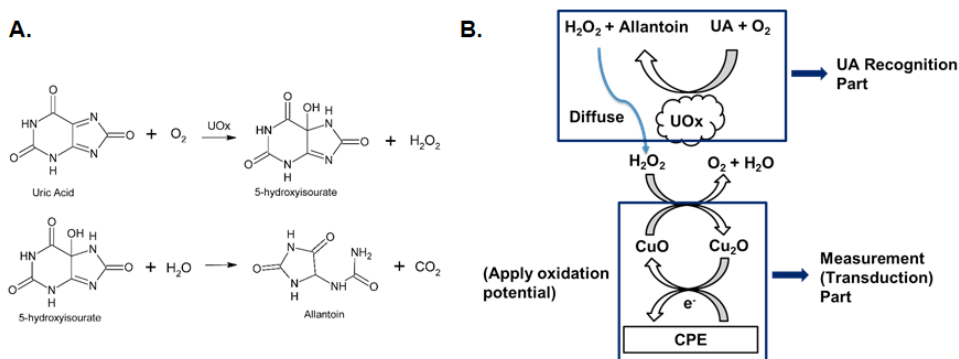


Figure 2. (A) Reaction scheme of enzymatic oxidation of UA by UOx. (B) Sensing mechanism for UA detection using UOx-CuO-CPE.

Electrochemical Response of UOx-CuO-CPE towards UA

In order to assess the viability of UOx-CuO-CPE for UA determination, CV measurements were done. Figure 3 shows the CV measurements of UA using CuO-CPE and UOx-CuO-CPE.

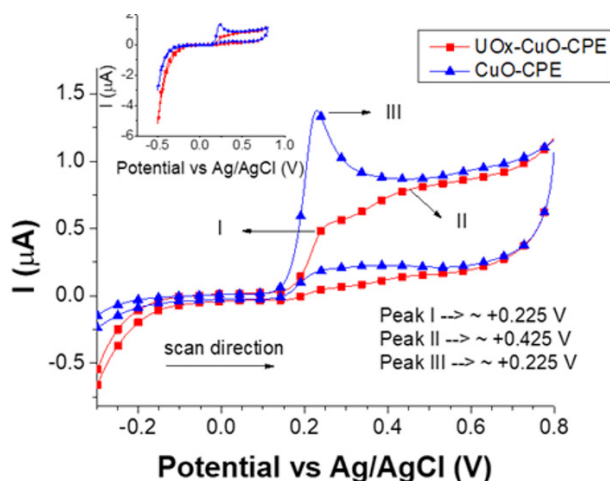


Figure 3. CV measurements of 79.4 μM UA in BBS (pH 9.0) using UOx-CuO-CPE (Cu deposition time: 25 s; Cu oxidation time: 125 s; UOx enzyme loading: 0.1 mg/mL) and CuO-CPE (Cu deposition time: 25 s; Cu oxidation time: 125 s). CV measurements were done at 10 mV/s scan rate. Insets show the whole CV curves.

The CV curve of UA using UOx-CuO-CPE showed two oxidation peaks at $\sim +0.225$ V (Peak I) and at $\sim +0.425$ V (Peak II). Presence of two peaks indicates that UA is oxidized in two different routes, i.e. non-enzymatic (direct electrochemical oxidation) and enzymatic. The non-enzymatic oxidation is known since reduced UA is an electroactive species with an oxidation half-reaction shown in figure 4. On the other hand, CuO-CPE showed only one oxidation peak for UA positioned at $\sim +0.225$ V (Peak III), which has similar peak position with Peak I using UOx-CuO-CPE. Thus, Peak I can be assigned to the direct electrochemical oxidation of UA. Peak II can then be assigned to enzymatic oxidation of UA.

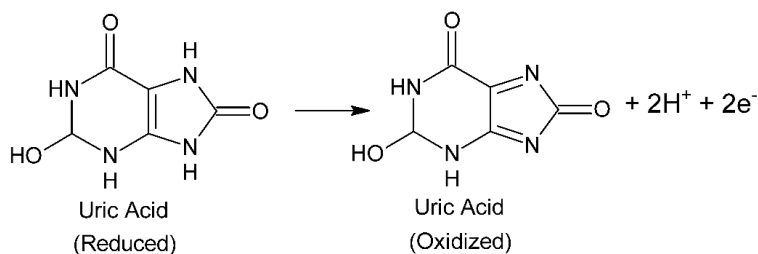


Figure 4. Oxidation half-reaction of UA.

Optimization of UOx-CuO-CPE Fabrication and Sensing Parameters

In order to obtain the highest sensitivity for UA sensing, different parameters were optimized including: (1) enzyme loading, (2) sensing solution pH, and (3) equilibration time. For the optimization of UOx enzyme loading, UOx-CuO-CPEs with different UOx enzyme loading were used for CV measurements of UA in BBS solution. Appendix Figure A1 shows the optimization of enzyme loading UOx-CuO-CPE and the CV curves of UA using fabricated UOx-CuO-CPEs with different enzyme loading. As shown in the figure, an increasing trend can be observed for Ave. Ip (for oxidation peaks corresponding to enzymatic oxidation of UA positioned at $\sim +0.410$ V) with increasing enzyme concentration from 0.02 mg/mL UOx to 0.3 mg/mL UOx. This can be attributed to the increase in the number of UOx units present on the electrode surface. Further increasing the UOx concentration dropcasted onto the electrode causes a significant drop in peak currents both for electrochemical oxidation of UA and Cu_2O . This can be due to an increase in non-conducting enzyme units on the electrode surface which hinders not only the direct electron transfer from UA, but also the diffusion of enzymatically produced H_2O_2 to the nearest CuO particle. From these observations, the optimized UOx concentration for the fabrication of UOx-CuO-CPE biosensor is 0.3 mg/mL.

For the optimization of sensing solution pH, equally fabricated UOx-CuO-CPEs were used to measure for CV measurements of UA in BBS solutions. Appendix Figure A2 shows the optimization graph for the sensing solution pH optimization and the CV curves of UA at different solution pH values using UOx-CuO-CPE.

As shown in the figure, the response of the UOx-CuO-CPE towards sensing solutions with pH 8.2 and pH 8.4 showed significantly small Ave. Ip for Cu_2O oxidation, indicating that at these pH values, the biosensor has low activity to produce H_2O_2 . Further increasing the pH to 8.6, the biosensor showed a significant increase in Ave. Ip for Cu_2O oxidation. Further increasing the sensing solution pH led to a significant decrease in peak current for Cu_2O oxidation. These observations are due to the fact that UA molecules are at monoionic form at pH 8.6, which are a natural substrate of UOx (Gabison et al. 2008). Increasing the pH will further deprotonize the UA, converting it to 3,9 – dianion form of UA, which is not the natural substrate of UOx.

For the optimization of equilibration time, equally fabricated UOx-CuO-CPEs were used to measure UA in BBS (pH 8.6) at different equilibration times via CV. Appendix Figure A3 shows the optimization graph for the equilibration time optimization and the CV curves of UA at different equilibration time using UOx-CuO-CPE. As shown in the figure, 3 minutes equilibration time showed the highest Ave. Ip.

Shorter equilibration times were observed to have low Ave. I_p , indicating low H_2O_2 production. Longer equilibration times resulted in decreased Ave. I_p , which was caused by increased production of allantoin that may competitively inhibit UA at the active site of UOx (Gabison et al. 2006). With these observations, the optimized equilibration time was chosen to be equal to 3 minutes. Table 1 summarizes the obtained value for different parameters that were obtained in this study.

Table 1. Optimized Parameters for UOx-CuO-CPE

Optimized Parameter	Optimized Value
Cu deposition time	20 s
Cu oxidation time	60 s
Enzyme loading	0.3 mg/mL
Sensing solution pH	pH 8.6
Equilibration time	3 mins

Electrochemical Characterization of CPE, CuO-CPE, and UOx-CuO-CPE

In the fabrication of UOx-CuO-CPE, UOx and CuO were used as modifiers on CPE and both can affect the overall surface conductivity of the resulting biosensor. In order to assess the effect of both CuO and UOx on the rate of electron transfer at the electrode–solution interface, CV and EIS measurements were done using CPE, CuO-CPE, and UOx-CuO-CPE. Figure 5 shows the CV curves, Nyquist plots, and circuit models using CPE, CuO-CPE, and UOx-CuO-CPE, on BBS (pH 8.6) with ferrocyanide $[Fe(CN)_6^{4-}]$ redox probe.

Figure 5 shows the CV and Nyquist plots using the CPE, CuO-CPE, and UOx-CuO-CPE on BBS (pH 8.6) with $Fe(CN)_6^{4-}$ redox probe. Figure 5A shows the CV curves of $Fe(CN)_6^{4-}$ using the three electrodes. Using CPE, typical reversible redox peaks with similar peak heights were observed owing to the conducting nature of MWCNT on the electrode surface. For CuO-CPE, a quasi-reversible redox peak was observed. The oxidation of $Fe(CN)_6^{4-}$ to $Fe(CN)_6^{3-}$ is more favored as indicated by a significantly lower reduction peak height as compared to oxidation peak height. For UOx-CuO-CPE, a significant decrease in peak heights for both reduction and oxidation peaks was observed. The decrease in peak heights can be attributed to the decrease in surface conductivity of the electrode due to the non-conducting nature of UOx.

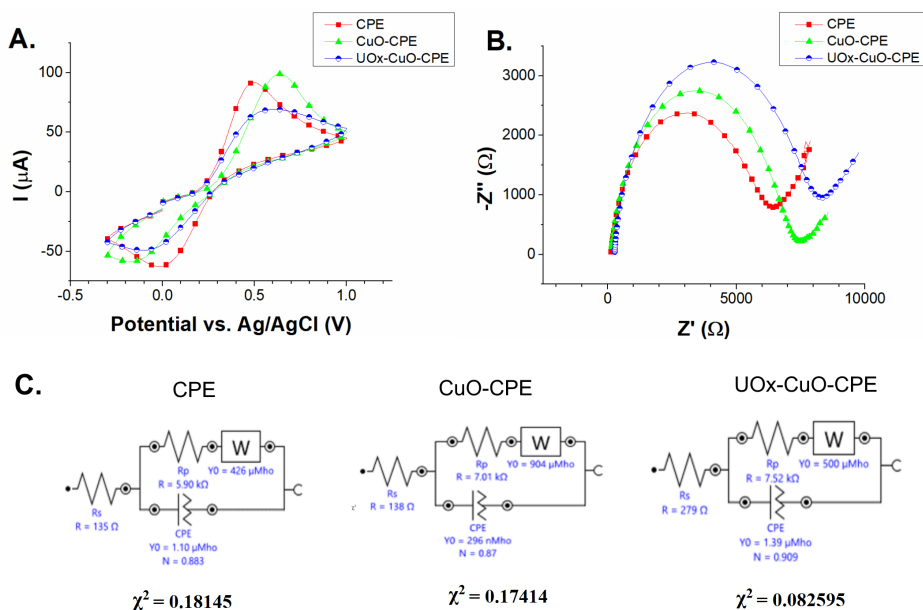


Figure 5. (A) CV curves and (B) Nyquist plots using CPE, CuO-CPE, and UOx-CuO-CPE. The solution used was 5 mM $\text{K}_4[\text{Fe}(\text{CN})_6]$ in BBS (pH 8.6). CV measurements were done at 10 mV/s scan rate. EIS measurements were done at frequency range 20 kHz–0.1 Hz at 0.35 V applied potential. (C) Circuit model from EIS measurements using CPE, CuO-CPE, and UOx-CuO-CPE. Chi-squared (χ^2) values for the curve fitting are shown.

As shown in figure 5B, Nyquist plots of the three electrodes indicate similar electrochemical cell properties in the presence of a redox probe. All of the electrodes were observed to have both electrochemical circles with linear portion at lower frequencies. Such pattern of a Nyquist plot can be modelled using Randles cell with Warburg impedance element as shown in figure 5C. The diameter of the electrochemical circle is equal to the charge transfer resistance (R_{ct}) or polarization resistance (R_p), which is directly related to the rate of electron transfer at the electrode-solution interface. Based on the circuit modelling, the R_{ct} of CPE, CuO-CPE, and UOx-CuO-CPE were determined to be at 5.90 k Ω , 7.01 k Ω , and 7.52 k Ω , respectively. The R_{ct} of CuO-CPE is significantly higher to the R_{ct} of CPE. This observation is in conformity with the CV measurements in figure 5A, where $\text{Fe}(\text{CN})_6^{4-}/\text{Fe}(\text{CN})_6^{3-}$ redox couple showed a quasi-reversible redox reaction using CuO-CPE. For UOx-CuO-CPE, its R_{ct} is significantly higher than the R_{ct} of both CPE and CuO-CPE. This observation can again be attributed to the non-conducting nature of UOx, which resulted in hindered direct electron transfer between $\text{Fe}(\text{CN})_6^{4-}$ and UOx-CuO-CPE.

Assessment of Biosensor Activity

In order to assess the biosensor activity, the apparent Michaelis constant (K_m^{app}) was determined via CV measurements of UA solutions with different UA concentrations using the optimized UOx-CuO-CPE. The K_m^{app} of UOx on the electrode surface was estimated using the Hanes-Woolf plot. Appendix Figure A4 shows the Hanes-Woolf plot for K_m^{app} determination and the CV curves for different UA concentrations used for the Hanes-Woolf plot. The K_m^{app} was determined at 41.5 μM . The calculated K_m^{app} for UOx-CuO-CPE is much lower than some of the previous reports on UA biosensor involving UOx (Jindal et al. 2012; Verma et al. 2019). Lower K_m^{app} is more favorable for an enzyme-based biosensor as it ensures enhanced affinity of the substrate to the immobilized enzyme which leads to enhanced response. This is due to the inverse relationship of K_m^{app} and reaction rate (v).

Aside from K_m^{app} , maximum velocity (V_{max}) of the biosensor was also determined using the Hanes-Woolf plot. The V_{max} gives information on the rate of enzymatic catalysis. The measured V_{max} of the UOx-CuO-CPE is at 6.93×10^{-5} μM UA detected/min. This is much lower than the reported UOx activity in free solution (for the same amount of UOx dropcasted onto the CuO-CPE surface) which is at 2.14×10^{-1} μM UA converted to allantoin/min. A possible reason for this observation is because UA molecules are limited only to diffuse towards the active sites of UOx that are facing the electrode-solution interface. Thus, UOx in free solution is more active than adsorbed UOx.

Determination of Analytical Merits for UA Sensing Using UOx-CuO-CPE and Differential Pulse Voltammetry (DPV) as Sensing Technique

DPV measurements for UA were done using the optimized value for different parameters as previously shown in table 1. A calibration curve was done by measuring different solutions of UA with varying UA concentrations. Figure 6 shows the calibration curve for UA detection using the fabricated UOx-CuO-CPE and the DPV curves of UA solutions with different concentrations using optimized UOx-CuO-CPE.

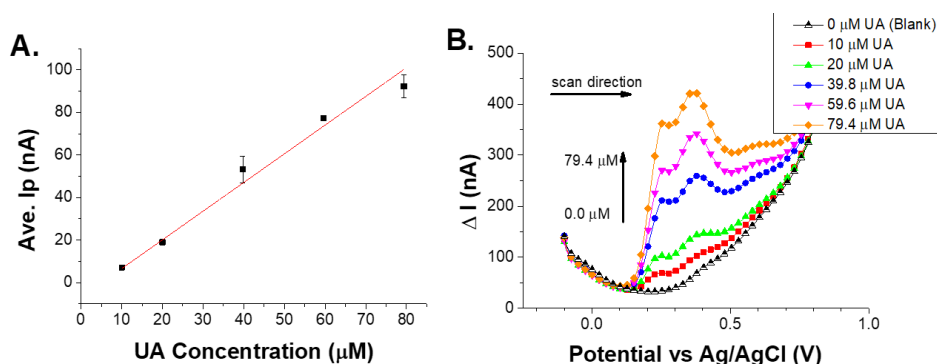


Figure 6. (A) Calibration curve for UA measurements using UOx-CuO-CPE. (B) DPV curves of UA in BBS (pH 8.6) with different UA concentration using UOx-CuO-CPE. Three (3) measurements were done for each UA concentration. Error bars represent standard deviation for three measurements. I_p for each DPV measurement was measured at around +0.370 V.

As shown in figure 6A, a linear correlation was found between UA concentration and Ave. I_p ranging from 10.0 μM to 79.4 μM ($R^2 = 0.9926$). The limit of detection (LOD) for UA detection using the UOx-CuO-CPE was determined at 8.82 μM . Table 2 shows the figures of merit for the UA measurement using UOx-CuO-CPE. Linear correlation analysis of the calibration curve was done. As shown in table 2, the R^2 value for the linear regression is equal to 0.9926, indicating linear correlation of Ave. I_p with UA concentration.

Table 2. Figures of merit for UA measurement using UOx-CuO-CPE

Figures of Merit	Value
Linear range	10.0 μM – 79.4 μM
Sensitivity	$1.348 \pm 0.067 \text{ nA}/\mu\text{M}$
Linearity (R^2)	0.9926
Limit of Detection (LOD)	8.82 μM
Limit of Quantification (LOQ)	29.39 μM

Assessment of UOx-CuO-CPE Selectivity

UOx is the molecular recognition element of the UOx-CuO-CPE biosensor for UA. Thus, the main purpose of UOx is to enhance the selectivity of the biosensor. In order to assess the selectivity of the fabricated biosensor, the electrochemical response of UOx-CuO-CPE towards possible interferences must first be studied. Different possible interferences were studied including the following: creatinine, xanthine, and glucose. Creatinine was included in this selectivity test because of

its presence in human urine as well as having a slight similarity in structure with UA. Xanthine was included in this selectivity test because of its high structural similarity with UA. Lastly, glucose was included in this selectivity test also because of its presence in urine. Urea was not included in this selectivity test because of its non-electroactive nature and it was shown in a previous study that urea did not significantly interfere with H_2O_2 measurements using CuO-CPE measurements (Buenaventura and Yago 2020). Figure 7 shows the CV curves for the mentioned compounds using UOx-CuO-CPE. From the figure, CV measurements of the studied interferences using UOx-CuO-CPE showed no appreciable oxidation peak at $\sim +0.4$ V. Among the studied interferences, only xanthine gave a significant oxidation peak located at $\sim +0.65$ V, which is far from the measurement potential ($\sim +0.4$ V) for UA.

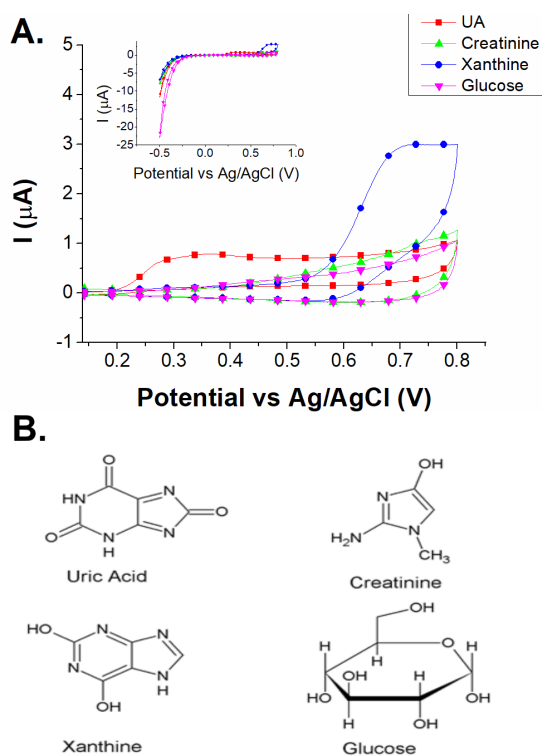


Figure 7. (A) CV curves of 39.6 μM UA, creatinine, xanthine, and glucose in BBS (pH 8.6), using UOx-CuO-CPE. (B) Chemical structures of UA, creatinine, xanthine, and glucose. Scan rate at 10 mV/s. Inset in (A) shows the whole CV curves.

To further assess the selectivity of UOx-CuO-CPE towards UA, different biomolecules (creatinine, xanthine, and glucose) were added into separate UA sensing solutions and were measured using UOx-CuO-CPE. Figure 8 shows the selectivity study for UOx-CuO-CPE in comparison with CPE. Based on figure 8A, UOx-CuO-CPE showed

no significant difference in its electrochemical response with UA when added with other biomolecules. This is confirmed by single factor Analysis of Variance (ANOVA) with calculated F (3.120) less than the F_{critical} (4.066). Appendix Table B1 shows the biosensor responses and the ANOVA table. For comparison, a selectivity study of CPE was also done. Figure 8B shows that there is a significant difference with the response of CPE towards UA alone as compared with added biomolecules. This is confirmed by single factor ANOVA with calculated F (16.355) larger than the F_{critical} (4.066). Appendix Table B2 shows the CPE responses and the ANOVA table. Therefore, the presence of creatinine, xanthine, and glucose do significantly affect the response of CPE towards UA. These results thus proved the effectiveness of the UOx enzyme as a molecular recognition element in the final biosensor. Appendix Figure A5 shows the DPV curves of UA, and UA with interferences, using UOx-CuO-CPE and CPE.

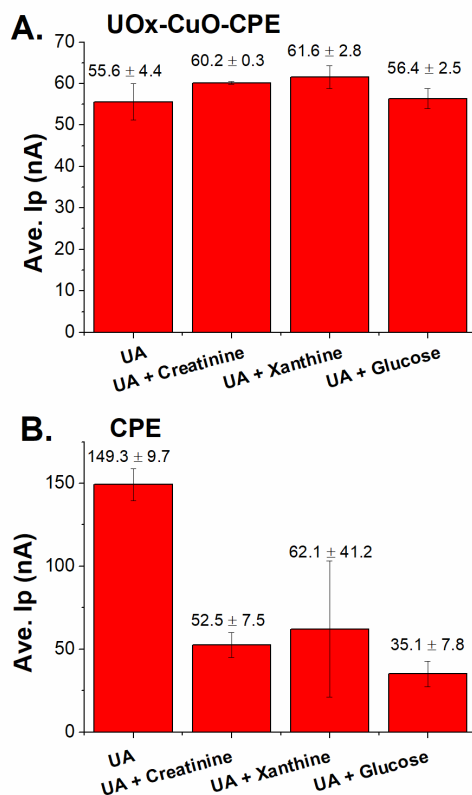


Figure 8. Selectivity study of UA determination via DPV using (A) UOx-CuO-CPE and (B) CPE. Three measurements ($n=3$) were done for each sensing solution combination. Measurement values are shown above the bars with the format: Average peak current (Ave. Ip) \pm standard deviation for three measurements. Ip for each DPV measurement was measured at around +0.370 V.

Assessment of UOx-CuO-CPE Reusability and Fabrication Repeatability Using UOx-CuO-CPE

In a chemical sensor/biosensor research, it is important also to assess the reusability as well as the fabrication repeatability of the sensor being developed. In this study, a sensor reusability test was done by measuring UA over several repetitions ($n=5$) using UOx-CuO-CPE. As shown in Appendix Table B3, the average response of UOx-CuO-CPE towards $79.4 \mu\text{M}$ UA is at 113.6 ± 3.7 nA. The % relative standard deviation (% RSD) was determined at 3.28%. For the fabrication repeatability, UA measurements were done using three separate UOx-CuO-CPEs. Figure 9 shows the fabrication repeatability graph for the UOx-CuO-CPEs. As shown in the figure, the biosensor responses did not differ significantly. This is confirmed by single factor ANOVA with calculated F (1.396), which is less than F_{critical} (5.143). Appendix Table B4 shows the biosensor responses and ANOVA table.

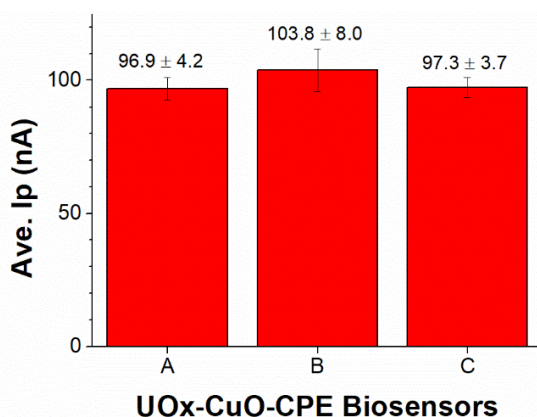


Figure 9. Biosensor fabrication repeatability study for UOx-CuO-CPE biosensors. Measurements for $79.4 \mu\text{M}$ UA in BBS (pH 8.6) were done using three separate UOx-CuO-CPE biosensors (labelled as A, B, and C). Three measurements ($n = 3$) were done for each biosensor. Measurement values are shown above the bars with the format: average peak current (Ave. Ip) \pm standard deviation for the three measurements. Ip for each CV measurement was measured at around +0.420 V.

Assessment of UOx-CuO-CPE Biosensor Stability

The stability of UOx-CuO-CPE was also studied to provide information about its usability after a certain period of storage. The UOx-CuO-CPE biosensor was tested for five-week stability in order to evaluate if it can give a similar response after storing it at a cold temperature ($\sim +4^\circ\text{C}$). Figure 10 compares the mean responses of the biosensor before (0^{th} week) and after five weeks (5^{th} week) of storage. As shown in the figure, UOx-CuO-CPE responses before and after five weeks of storage did

not differ significantly. This is confirmed by a two-sample t-test with calculated t equals to 0.156, which is smaller than the t_{crit} ($df = 2$, $\alpha = 0.05$) which is equal to 4.303. Appendix Table B5 shows the biosensor responses as well as t-test summary.

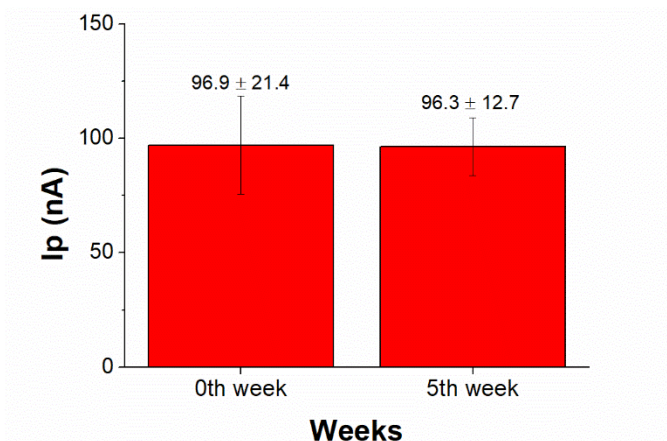


Figure 10. Five-week biosensor stability test. Three (3) measurements for $79.4 \mu\text{M}$ UA in BBS (pH 8.6) were done for each data set. Measurement values are shown above the bars with the format: average peak current (Ave. I_p) \pm standard deviation for three measurements. I_p for each CV measurement was measured at around +0.450 V.

Assessment of Applicability of UOx-CuO-CPE on Human Urine Using Synthetic Human Urine

In order to evaluate the effect of the matrix of human urine towards the UA measurement using UOx-CuO-CPE, a recovery test was performed. Table 3 shows the results of the recovery test for three spiking levels ($7.4 \mu\text{M}$, $30 \mu\text{M}$, and $55.8 \mu\text{M}$). As shown in the table, the recoveries for three spiking levels range from 90.27% to 102.3% with an RSD of not more than 2.55%, indicating that UOx-CuO-CPE is applicable for the quantification of UA in human urine. Appendix Figure A6 shows the DPV measurements of non-spiked and spiked synthetic urine.

Table 3. Recovery test for UOx-CuO-CPE using synthetic urine

Sample	Detected (μM)	Added (μM)	Found (μM)	Recovery	RSD (n=3)
1	$0.00 \pm 0.00^*$	7.40	7.55 ± 0.19	102.03%	2.55%
2	$0.00 \pm 0.00^*$	30.00	27.08 ± 0.28	90.27%	1.05%
3	$0.00 \pm 0.00^*$	55.80	52.01 ± 0.30	93.21%	0.59%

*No observable peaks

Comparison of UOx-CuO-CPE with Other Reported UOx-Based Biosensors

Table 4 shows the analytical performance of other reported UOx-based UA biosensors as compared with the fabricated UOx-CuO-CPE. Comparing UOx-CuO-CPE with other reported biosensors, the UOx-CuO-CPE biosensor has relatively low LOD and K_m^{app} . In particular, UOx-CuO-CPE showed a significant improvement in performance compared to UOx/CuO/Pt (Jindal et al. 2012). It also has lower K_m^{app} compared to UOx/Au-rGO/ITO (Verma et al. 2019) despite having a more sophisticated electrode modifier. This improved performance of UOx-CuO-CPE can be attributed to several factors including: 1) the use of CPE that is based on MWCNT (a highly conducting carbon allotrope (Jacobs et al. 2010)), and 2) the use of the dropcast method of enzyme depositing rather than covalent attachment of enzyme which can lower the activity of an enzyme (Feng and Ji 2011). Thus, the advantage of UOx-CuO-CPE, aside from having facile steps of fabrication, is good analytical performance for UA determination.

Table 4. Analytical performance of reported UOx-based electrochemical biosensors for UA compared to UOx-CuO-CPE

Enzyme-based Electrochemical Biosensor	Electrochemical Technique of Detection	Linear Range	Limit of Detection	Apparent Michaelis Constant (K_m^{app})	Reference
UOx/CuO/Pt	Amperometry	50 μ M – 1 mM	140 μ M	0.12 mM	(Jindal et al. 2012)
Nafion/UOx-HRP-mesoporous silica/GCE	Amperometry	2 μ M – 12 μ M	0.33 μ M	--	(Mundaca-Uribe et al. 2014)
Nafion/UOx/ZnO nanosheets/Ag/Si	Amperometry	50 μ M – 2 mM	0.019 μ M	0.026 mM	(Ahmad et al. 2015)
Graphene Oxide – Uox/GCE	Amperometry	20 μ M – 491 μ M	3.45 μ M	--	(Omar et al. 2016)
UOx/poly(4-aminosalicylic acid)/Prussian blue/ carbon graphite electrode	Amperometry	10 μ M – 200 μ M	3.0 μ M	--	(da Cruz et al. 2017)
UOx/Bull Serum Albumin (BSA)/BLG-MWCNTs-PtNPs/Glassy Carbon (GC) electrode	Amperometry	0.02 mM – 0.5 mM	0.8 μ M	--	(Han et al. 2019)
UOx/Au-rGO/ITO	Differential Pulse Voltammetry	50 μ M – 800 μ M	7.32 μ M	51.75 μ M	(Verma et al. 2019)
UOx-CuO-CPE	Differential Pulse Voltammetry	10.0 μ M – 79.4 μ M	8.82 μ M	41.46 μ M (0.0415 mM)	This work

CONCLUSION

An electrochemical enzyme-based biosensor for UA determination was developed and optimized in this study. A carbon paste electrode (CPE) and its pretreatment, which were previously optimized by our group in separate studies (Buenaventura et al. 2016; Buenaventura and Yago 2018), was modified further with CuO particles and a UOx enzyme to fabricate a biosensor that is sensitive and selective towards UA. CV measurements proved the retention of the capability of the UOx enzyme to catalyze UA oxidation after being dropcasted on the surface of CuO-CPE. The presence of UOx on the UOx-CuO-CPE resulted in an increase in R_{ct} as compared to CuO-CPE and CPE due to the non-conducting nature of UOx. Several parameters, including UOx enzyme loading, sensing solution pH, and equilibration time, were optimized. DPV measurements of UA using UOx-CuO-CPE showed a linear correlation between I_p and UA concentration. The LOD for UA measurement using UOx-CuO-CPE was determined at 8.82 μ M. UOx-CuO-CPE showed improved performance over some reported studies, which mainly could be due to the use of MWCNT-based CPE and the use of a non-covalent approach of immobilizing the UOx onto the electrode surface. Because of the presence of UOx as a selective modifier, UOx-CuO-CPE was also proven to be selective towards UA even in the presence of creatinine, xanthine, and glucose. Furthermore, UOx-CuO-CPE was also proven to be reusable, reproducible, and stable even after five weeks of storage. Results of a recovery test confirmed the applicability of UOx-CuO-CPE for UA determination in human urine.

ACKNOWLEDGMENTS

This research was supported by the Natural Sciences Research Institute (NSRI) of the University of the Philippines Diliman [CHE-17-1-01] and the Department of Science and Technology (DOST), Philippines.

REFERENCES

- Ahmad R, Tripathy N, Jang NK, Khang G, Hahn Y-B. 2015. Fabrication of highly sensitive uric acid biosensor based on directly grown ZnO nanosheets on electrode surface. *Sens Actuators B Chem.* 206:146-151.
- Arslan F. 2008. An amperometric biosensor for uric acid determination prepared from uricase immobilized in polyaniline-polypyrrole film. *Sensors (Basel, Switzerland).* 8(9):5492-5500.
- Ben-Ishay D, Dreyfuss F, Ullmann TD. 1961. Fanconi syndrome with hypouricemia in an adult: family study. *Am J Med.* 31(5):793-800.

- Bickel C, Rupprecht HJ, Blankenberg S, Rippin G, Hafner G, Daunhauer A, Hofmann K-P, Meyer J. 2002. Serum uric acid as an independent predictor of mortality in patients with angiographically proven coronary artery disease. *Am J Cardiol.* 89(1):12-17.
- Bravo R, Hsueh C, Brajter-Toth A, Jaramillo A. 1998. Possibilities and limitations in miniaturized sensor design for uric acid. *Analyst.* 123(7):1625-1630.
- Buenaventura AG, Lopez R, Yago AC. 2016. Carbon nanotube – polydimethylsiloxane paste electrodes as voltammetric sensor for ascorbic acid. Presented in 16th International Meeting on Chemical Sensors (IMCS 2016) (Oral).
- Buenaventura AG, Yago AC. 2020. Electrochemical reversible copper oxide (CuO) system on multiwalled carbon nanotube paste electrode (CPE) as sensor for hydrogen peroxide in wound cleaning solution. *Philipp J Sci.* 149(3-a):801-813.
- Buenaventura AGE, Yago ACC. 2018. Facile electrochemical pretreatment of multiwalled carbon nanotube - polydimethylsiloxane paste electrode for enhanced detection of dopamine and uric acid. *AIP Conference Proceedings.* 1958(1):020029.
- Chaudhari RD, Joshi AB, Srivastava R. 2012. Uric acid biosensor based on chemiluminescence detection using a nano-micro hybrid matrix. *Sens Actuators B Chem.* 173:882-889.
- da Cruz FS, Paula FdS, Franco DL, dos Santos WTP, Ferreira LF. 2017. Electrochemical detection of uric acid using graphite screen-printed electrodes modified with Prussian blue/poly(4-aminosalicylic acid)/uricase. *J Electroanal Chem.* 806:172-179.
- Desideri G, Castaldo G, Lombardi A, Mussap M, Testa A, Pontremoli R, Punzi L, Borghi C. 2014. Is it time to revise the normal range of serum uric acid levels? *Eur Rev Med Pharmacol Sci.* 18(9):1295-1306.
- Feig DI, Johnson RJ. 2003. Hyperuricemia in childhood primary hypertension. *Hypertension.* 42(3):247.
- Feng W, Ji P. 2011. Enzymes immobilized on carbon nanotubes. *Biotechnol Adv.* 29(6):889-895.
- Gabison L, Chiadmi M, Colloc'h N, Castro B, El Hajji M, Prangé T. 2006. Recapture of [S]-allantoin, the product of the two-step degradation of uric acid, by urate oxidase. *FEBS Lett.* 580(8):2087-2091.
- Gabison L, Prangé T, Colloc'h N, El Hajji M, Castro B, Chiadmi M. 2008. Structural analysis of urate oxidase in complex with its natural substrate inhibited by cyanide: mechanistic implications. *BMC Struct Biol.* 8(1):32.

- Han B, Pan M, Liu X, Liu J, Cui T, Chen Q. 2019. Electrochemical detection for uric acid based on β -lactoglobulin-functionalized multiwall carbon nanotubes synthesis with PtNPs nanocomposite. *Materials (Basel, Switzerland)*. 12(2):214.
- Ishizaka N, Ishizaka Y, Toda E-I, Nagai R, Yamakado M. 2005. Association between serum uric acid, metabolic syndrome, and carotid atherosclerosis in Japanese individuals. *Arterioscler Thromb Vasc Biol*. 25(5):1038.
- Jacobs CB, Peairs MJ, Venton BJ. 2010. Review: carbon nanotube based electrochemical sensors for biomolecules. *Anal Chim Acta*. 662(2):105-127.
- Jindal K, Tomar M, Gupta V. 2012. CuO thin film based uric acid biosensor with enhanced response characteristics. *Biosens Bioelectron* 38(1):11-18.
- Kay NE, Gottlieb AJ. 1973. Hypouricemia in Hodgkin's disease. Report of an additional case. *Cancer*. 32(6):1508-1511.
- Khan LB, Read HM, Ritchie SR, Proft T. 2017. Artificial urine for teaching urinalysis concepts and diagnosis of urinary tract infection in the medical microbiology laboratory. *J Microbiol Biol Educ*. 18(2):18.2.46.
- Masuo K, Kawaguchi H, Mikami H, Ogihara T, Tuck ML. 2003. Serum uric acid and plasma norepinephrine concentrations predict subsequent weight gain and blood pressure elevation. *Hypertension*. 42(4):474.
- Matsuura F, Yamashita S, Nakamura T, Nishida M, Nozaki S, Funahashi T, Matsuzawa Y. 1998. Effect of visceral fat accumulation on uric acid metabolism in male obese subjects: visceral fat obesity is linked more closely to overproduction of uric acid than subcutaneous fat obesity. *Metabolism*. 47(8):929-933.
- Mundaca-Urbe R, Bustos-Ramírez F, Zaror-Zaror C, Aranda-Bustos M, Neira-Hinojosa J, Peña-Farfal C. 2014. Development of a bienzymatic amperometric biosensor to determine uric acid in human serum, based on mesoporous silica (MCM-41) for enzyme immobilization. *Sens Actuators B Chem*. 195:58-62.
- Nakanishi N, Okamoto M, Yoshida H, Matsuo Y, Suzuki K, Tatara K. 2003. Serum uric acid and risk for development of hypertension and impaired fasting glucose or type II diabetes in Japanese male office workers. *Eur J Epidemiol*. 18(6):523-530.
- Obermayr RP, Temml C, Gutjahr G, Knechtelsdorfer M, Oberbauer R, Klauser-Braun R. 2008. Elevated uric acid increases the risk for kidney disease. *J Am Soc Nephrol*. 19(12):2407-2413.
- Omar MN, Salleh AB, Lim HN, Ahmad Tajudin A. 2016. Electrochemical detection of uric acid via uricase-immobilized graphene oxide. *Anal Biochem*. 509:135-141.

Perez-Ruiz F, Dalbeth N, Bardin T. 2015. A review of uric acid, crystal deposition disease, and gout. *Adv Ther.* 32(1):31-41.

Puig JG, Mateos AF, Gaspar G, Martinez EM, Ramos T, Lesmes A. 1984. Hypouricemia and medullary carcinoma of the thyroid. In: De Bruyn CHMM, Simmonds HA, Müller MM, editors. *Purine metabolism in man-IV: part a: clinical and therapeutic aspects; regulatory mechanisms.* Boston (MA): Springer US. p. 211-213.

Rafati AA, Afraz A, Hajian A, Assari P. 2014. Simultaneous determination of ascorbic acid, dopamine, and uric acid using a carbon paste electrode modified with multiwalled carbon nanotubes, ionic liquid, and palladium nanoparticles. *Microchim Acta.* 181(15):1999-2008.

Suki WN, Massry SG. 2012. *Therapy of renal diseases and related disorders.* NY: Springer US.

Usman Ali SM, Alvi NH, Ibupoto Z, Nur O, Willander M, Danielsson B. 2011. Selective potentiometric determination of uric acid with uricase immobilized on ZnO nanowires. *Sens Actuators B Chem.* 152(2):241-247.

Verma S, Choudhary J, Singh KP, Chandra P, Singh SP. 2019. Uricase grafted nanoconducting matrix based electrochemical biosensor for ultrafast uric acid detection in human serum samples. *Int J Biol Macromol.* 130:333-341.

Walker HK, Hall WD, Hurst JW. 1990. *Clinical methods: the history, physical, and laboratory examinations.* 3rd ed. Boston: Butterworths.

Wang Y, Xu H, Zhang J, Li G. 2008. Electrochemical sensors for clinic analysis. *Sensors.* 8(4).

Watts RWE. 1974. Determination of uric acid in blood and in urine. *Ann Clin Biochem.* 11(1-6):103-111.

Wu D, Lu H-F, Xie H, Wu J, Wang C-M, Zhang Q-L. 2015. Uricase-stimulated etching of silver nanoprisms for highly selective and sensitive colorimetric detection of uric acid in human serum. *Sens Actuators B Chem.* 221:1433-1440.

Zhang T, Sun X, Liu B. 2011. Synthesis of positively charged CdTe quantum dots and detection for uric acid. *Spectrochimica Acta Part A: Spectrochim Acta A Mol Biomol Spectrosc.* 79(5):1566-1572.

—

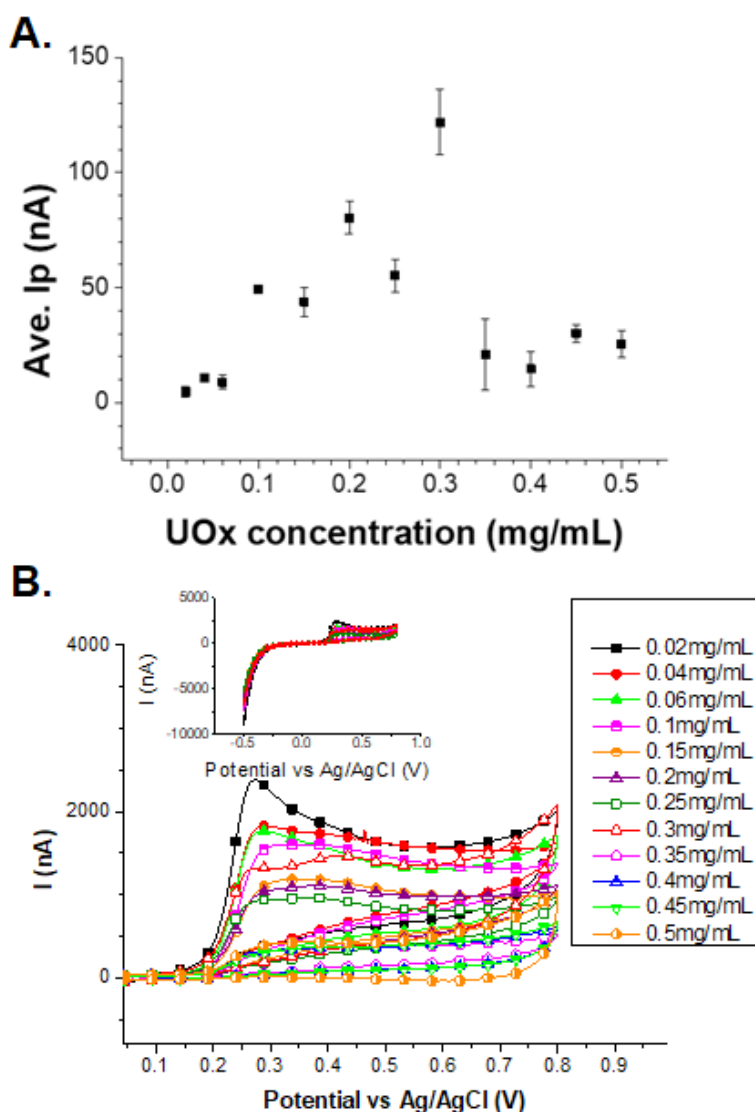
Allan Christopher C. Yago <acyago@up.edu.ph> is currently an Associate Professor in the Institute of Chemistry UP Diliman. He took his B.S., M.S., and Ph.D. in Chemistry in the Institute of Chemistry, UP Diliman, from 2001 to 2014. His main research interests are on the preparation and characterization of sensor materials from polymers, nanoparticles, and composites, electrochemistry and electro-analytical methods, molecular imprinting on polymers, and anti-corrosion coatings. He heads the Sensor Materials Development (SMD) lab located in IC Research building room 321-322.

Angelo Gabriel E. Buenaventura is currently a Research Assistant in the Institute of Chemistry UP Diliman. He took his M.S. Chemistry degree in the Institute of Chemistry, UP Diliman, from 2015 to 2020. He got his B.S. Chemistry degree in the College of Science, University of Santo Tomas, from 2010 to 2014. His main research interest is on the development and fabrication of chemical sensors and biosensors for various chemicals including environmental pollutants and important health – related biochemical compounds.

Appendix Figure A1

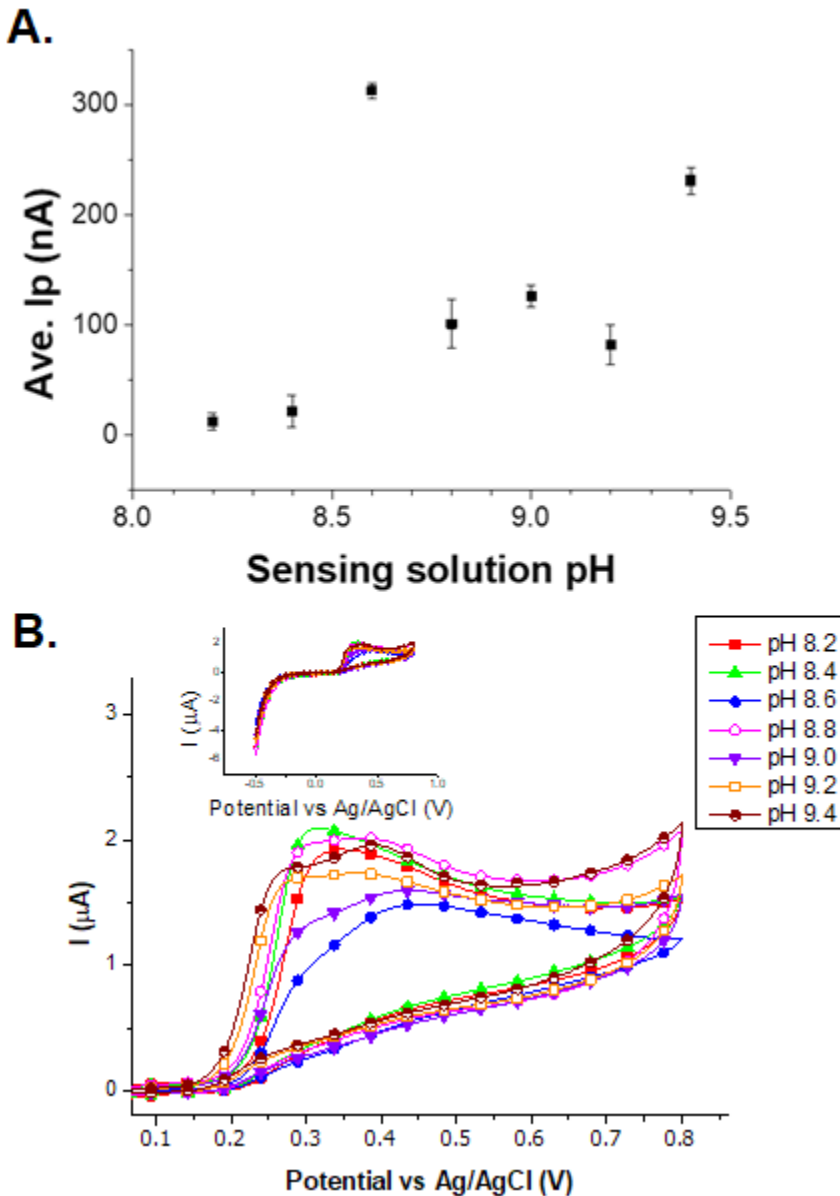
(A) Optimization graph for UOx loading optimization. Three (3) measurements were done for each enzyme concentration. Error bars represent standard deviation for three measurements. Peak currents (I_p) were measured at $E_p = \sim +0.410$ V. (B) CV curves of $79.4 \mu\text{M}$ UA in BBS (pH 9.0) using UOx-CuO-CPEs which were fabricated by drop casting UOx solution with different UOx concentrations; scan rate at 10 mV/s , 3 minutes equilibration time, 20 s Cu deposition time, 60 s Cu oxidation time.

Inset shows the whole CV curves.



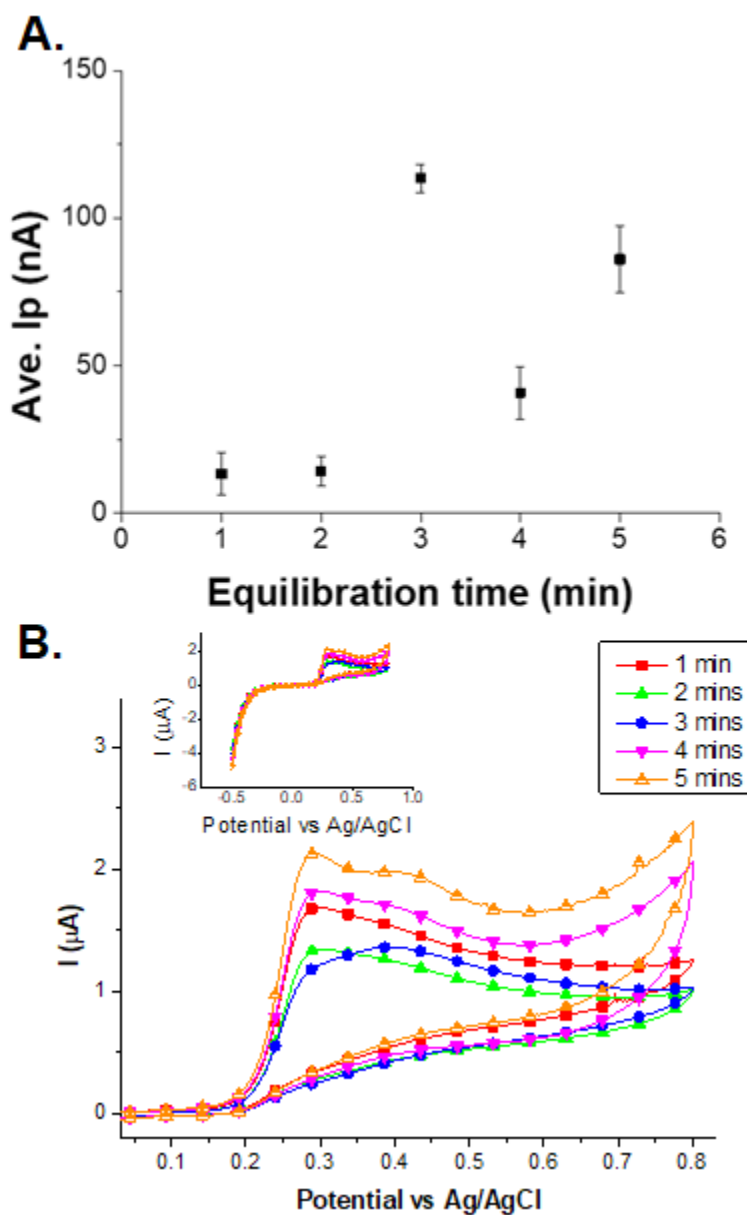
Appendix Figure A2

(A) Optimization graph for Sensing solution pH. Three (3) measurements were done for each pH. Error bars represent standard deviation for three measurements. I_p for each CV measurement was measured at around +0.400 V. (B) CV curves of 79.4 μM UA in BBS (varying pH) using UOx-CuO-CPE; scan rate at 10 mV/s, 3 minutes equilibration time, 20 s Cu deposition time, 60 s Cu oxidation time, 0.3 mg/mL enzyme loading. Inset shows the whole CV curves.



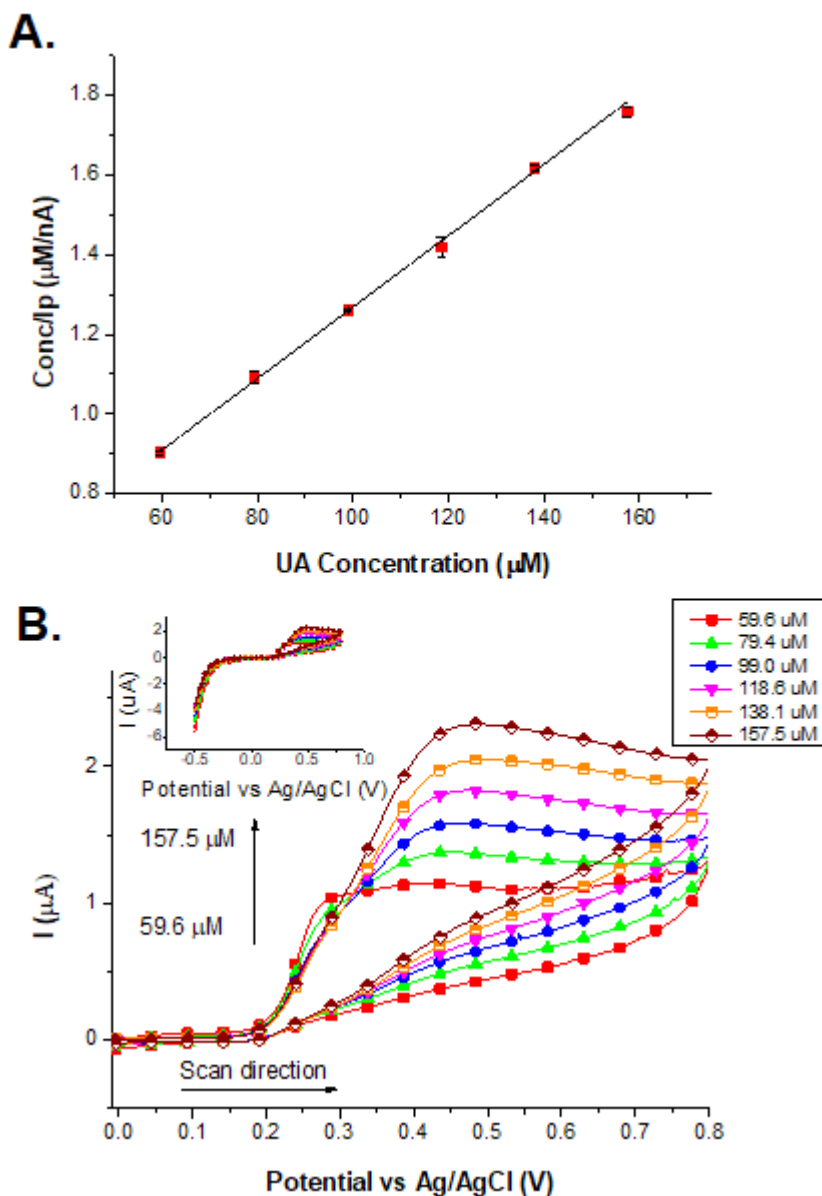
Appendix Figure A3

(A) Optimization graph for equilibration time. Three (3) measurements were done for each equilibration time. Error bars represent standard deviation for three measurements. I_p for each CV measurement was measured at around +0.400 V. (B) CV curves of 79.4 μM UA in BBS (pH 8.6) using UOx-CuO-CPE; scan rate at 10 mV/s, varying equilibration time, 20 s Cu deposition time, 60 s Cu oxidation time, 0.3 mg/mL enzyme loading. Inset shows the whole CV curves.



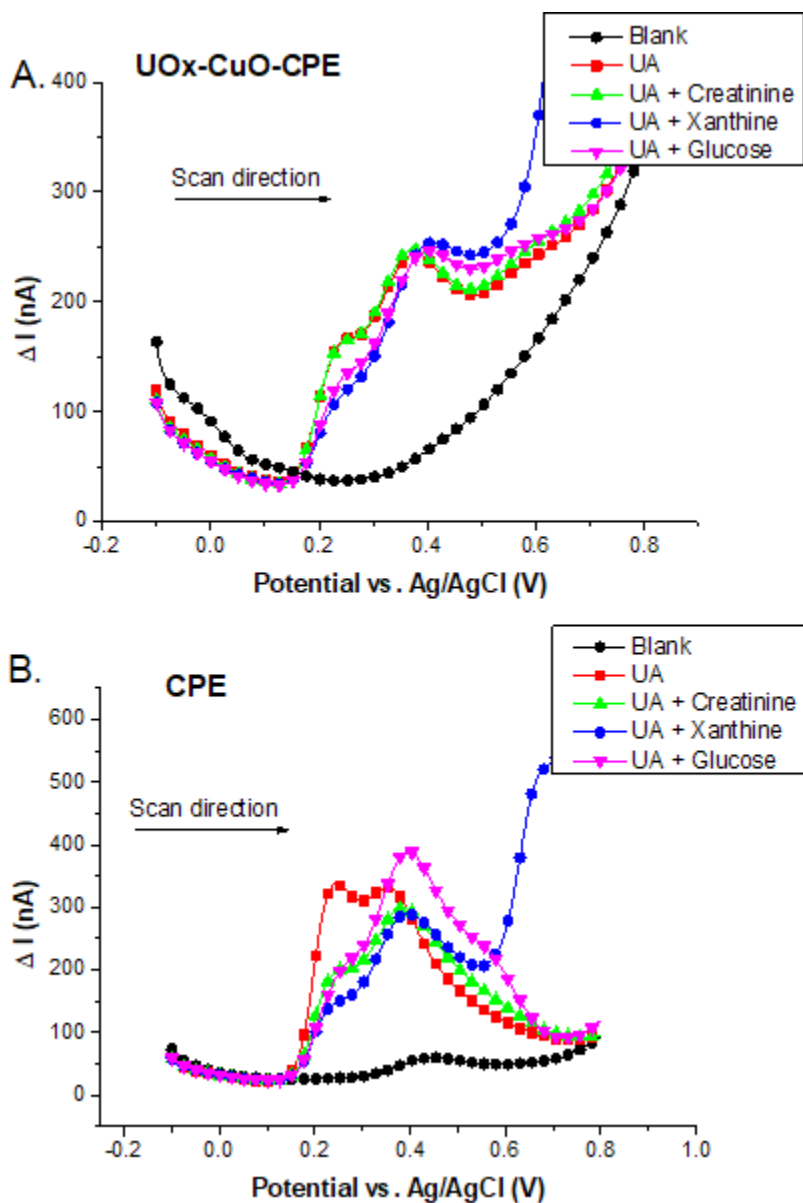
Appendix Figure A4

(A) Hanes-Woolf plot for determination of K_m^{app} . Three (3) measurements were done for each UA concentration. Error bars represent standard deviation for three measurements. I_p for each CV measurement was measured at around +0.400 V. (B) CV plots of solutions with different UA concentration using UOx-CuO-CPE; scan rate at 50 mV/s. Inset shows the whole CV curves.



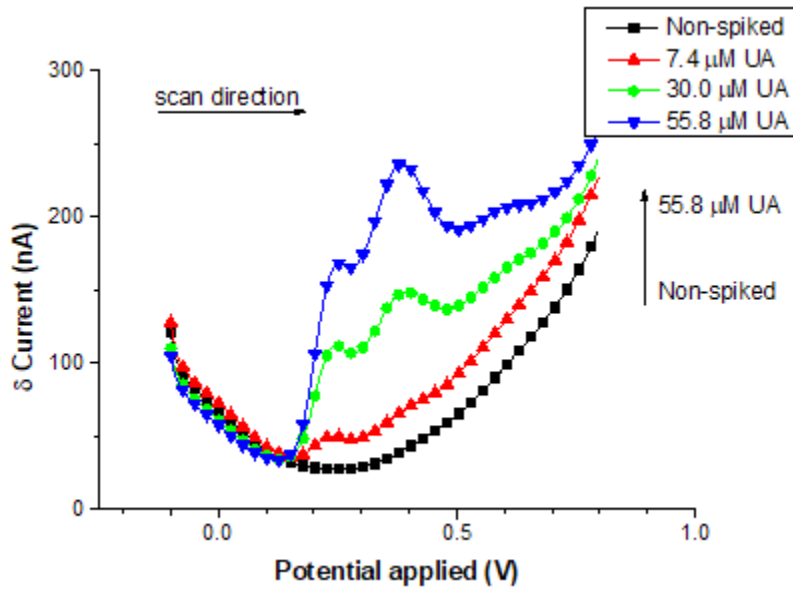
Appendix Figure A5

DPV curves of Blank (BBS; pH 8.6), UA, UA + creatinine, UA + xanthine, and UA + glucose, using UOx-CuO-CPE (A) and CPE (B).



Appendix Figure A6

DPV curves of non-spiked synthetic urine sensing solution and synthetic urine sensing solutions spiked with varying amounts of UA; UOx-CuO-CPE was used as working electrode.



Appendix Table B1

UOx-CuO-CPE electrochemical response values for different sensing solution combinations and single factor ANOVA Table

UOx-CuO-CPE electrochemical responses

Sensing Solution	Trial 1	Trial 2	Trial 3	Average
UA	5.06E+01	5.81E+01	5.82E+01	55.62033
UA + Creatinine	6.05E+01	6.03E+01	5.98E+01	60.19333
UA + Xanthine	6.43E+01	6.03E+01	5.98E+01	61.47167
UA + Glucose	5.37E+01	5.69E+01	5.86E+01	56.384

Single factor ANOVA

Source of Variation	SS	df	MS	F	P-value	F critical
Between Groups	73.32234	3	24.44078	3.119790847	0.088047	4.066181
Within Groups	62.67287	8	7.834109			
Total	135.9952	11				

Appendix Table B2

CPE electrochemical response values for different sensing solution combinations and single factor ANOVA Table

CPE electrochemical responses				
Sensing Solution	Trial 1	Trial 2	Trial 3	Average
UA	1.58E+02	1.39E+02	1.52E+02	149.3333
UA + Creatinine	4.42E+01	5.48E+01	5.86E+01	52.55067
UA + Xanthine	1.09E+02	4.33E+01	3.38E+01	62.14367
UA + Glucose	4.41E+01	3.05E+01	3.07E+01	35.06833

Single factor ANOVA						
Source of Variation	SS	df	MS	F	P-value	F critical
Between Groups	23367.11	3	7789.036	16.355	0.0008956	4.066181
Within Groups	3809.983	8	476.2479			
Total	27177.09	11				

Appendix Table B3Peak current (I_p) for several trials of UA measurement using UOx-CuO-CPE

Trials	I_p (nA)
1	111.7
2	111.4
3	115.8
4	119.0
5	110.0
Ave I_p	113.6
SD (n=5)	3.7
% RSD	3.28

*CV technique was used

** I_p was measured for each CV measurement at around +0.410 V

Appendix Table B4

UOx-CuO-CPEs electrochemical responses towards UA and single-factor ANOVA Table

UOx-CuO-CPE electrochemical responses

Biosensor	Trial 1	Trial 2	Trial 3	Average
A	9.40E+01	1.13E+02	1.01E+02	96.95367
B	9.51E+01	9.72E+01	9.61E+01	103.8063
C	1.02E+02	1.02E+02	9.44E+01	97.32

Single factor ANOVA

Source of Variation	SS	df	MS	F	P-value	F critical
Between Groups	89.16576	2	44.58288	1.396001	0.317827	5.143253
Within Groups	191.6169	6	31.93614			
Total	280.7826	8				

Appendix Table B5

UOx-CuO-CPE electrochemical responses for UA before and after 5 weeks of storage and t-test summary

UOx-CuO-CPE Responses

Trial	0th week Ip (nA)	5th week Ip (nA)
1	2.40E+02	1.90E+02
2	2.06E+02	2.13E+02
3	2.00E+02	2.11E+02

T-test summary

	0th week Ip (nA)	5th week Ip (nA)	Difference
Average	2.15E+02	2.05E+02	1.07E+01
SD	21.44285	12.6609281	
SD²	459.7956	160.2991	
SD²/N	153.2652	53.4330333	
df	2		
t	0.747		
t crit (95%)	4.303		